Environ Earth Sci (2016) 75:706
DOI 10.1007/s12665-016-5533-5

ORIGINAL ARTICLE

Prediction of water-inrush risk areas in process of mining under the unconsolidated and confined aquifer: a case study from the Qidong coal mine in China

Luwang Chen[1] · Xiaoqing Feng[1] · Wenping Xie[1] · Dongqing Xu[1]

Received: 1 August 2015 / Accepted: 3 March 2016 / Published online: 13 April 2016

Abstract The unconsolidated Cenozoic formation is well developed in the Qidong coal mine. Water-inrushes from the bottom unconsolidated Cenozoic aquifer, which is the confined aquifer, have happened several times during mining in the north mining area of the Qidong coal mine. To predict the water-inrush risk areas in the south mining area of the Qidong coal mine where some working faces have just begun to mine, the engineering analogy method is used on basis of the Fisher's discriminant model from the actual mining situation in the north mining area. Six main influence factors including the effective thickness, the specific yield, and the load transfer coefficient of the aquifer, the effective thickness of the protective bedrock layer, the fractal dimensional value of bedrock faults and the distance between the key hard stratum and the primary mineable coal seam are selected as discriminant indexes, and their corresponding data in the north mining area of the Qidong coal mine are served as training samples. On this basis, the Fisher's discriminant model for water-inrush is established and water-inrush risk areas including the safety, the medium risk and the risk areas of no. 6_1, 8_2 and 9 primary mineable coal seams in the south mining area of the Qidong coal mine are predicted by the model. The model's accuracy is 90.4 %, the scatter diagram of training samples shows obviously classified effect and the field verification indicates that the predicted type is consistent with the actual type. Results show that the discriminant model is well applied in the engineering analogy method and the water-inrush risk areas predicted by the discriminant model contribute to the subsequent mining in the south mining area in the Qidong coal mine.

Keywords Unconsolidated and confined aquifer · Water-inrush risk area · Fisher's discriminant analysis · Engineering analogy

✉ Xiaoqing Feng
hpfeng35@163.com

Luwang Chen
luwangchen8888@163.com

[1] School of Resources and Environmental Engineering, Hefei University of Technology, No. 193 of Tunxi Road, Hefei 230009, China

Introduction

In China, a considerable number of coal seams are covered by the unconsolidated Cenozoic formation, which is comprised of clay, sand, gravel, and so on, in the Yellow River and the Huai River alluvial plain areas (Zhang and Peng 2005). Usually, at the bottom of the unconsolidated formation, a confined aquifer develops with water-bearing sand and gravel, which is a potential threat to safe mining due to water-inrush (Chen et al. 2014). The statistics shows that about 285 coal mines (with estimated reserves exceeding 100 billion tons) of 600 in China suffer from water-inrush during extracting the coal seams covered by the unconsolidated Cenozoic formation.

Such water-inrush presents many concerns for miners and researchers (Hill and Price 1983; Booth 1986; Kim et al. 1997; Islam et al. 2009). In order not to destroy the groundwater environment in the unconsolidated formation, an aquifer protection extracting technique is applied in the western mine areas in China, which will enable the mining-induced dropdown level of the groundwater to be restored to its original level (Zhang et al. 2011). Whether the dropdown level can be well restored depends not only on some geological conditions including the presence of severely weathered bedrocks, weak strata and their locations, but also the groundwater recharge rate and the mining water inflow. Practical experience has proven that the dropdown level can recover by the protection extracting technique under some suitable geological conditions within a certain period although the aquifer may have been disturbed by mining (Booth and Spande 1992; Booth and Bertsch 1999; Booth et al. 2000). However, the technique will consume much coal resource, especially in the eastern mine areas in China where the coal resource is almost exhausted and the residual resource is commonly covered by the unconsolidated Cenozoic formation. To enhance the recovery and decrease resource loss, it is often necessary to extract the coal seams by maintaining rock and coal pillar as long as the mining does not suffer from water-inrush.

The height of rock and coal pillar is defined as the shortest vertical distance between the unconsolidated and confined aquifer and the working face (Zhang and Peng 2005; Miao et al. 2011). If the height is too small, the working face is very close to the confined aquifer and water-inrush from the confined aquifer will cause serious consequences such as mine inundation, endangering the lives of miners, and surface collapse. If the height is too large, it will lead to a loss of coal resource although the confined aquifer has no great threats to the working face, which is far from the confined aquifer. To liberate the coal resource under the aquifer as much as possible, many coal mines have tried to reduce the height of rock and coal pillar. However, with the expansion of the mining scale and the reduction of the height of rock and coal pillar, water-inrush under the aquifer happens from time to time, resulting in serious geological hazards and hindering the safe mining in coal mines (Wu et al. 2014, 2015; Zhang and Shen 2004).

In recent years, a variety of research methods have been applied to water-inrush hazards from the unconsolidated and confined aquifer. Based on the overlapping theory of multiple geological information, the "three maps—two predictions" method is put forward to evaluate water-inrush in process of mining under the unconsolidated and confined aquifer (LaMoreaux et al. 2014; Wu and Zhou 2008). In view of the high pressure in the unconsolidated and confined aquifer, the risk coefficient of water-inrush is proposed to evaluate the mining danger and to confirm the height of rock and coal pillars reasonably (Meng et al. 2013). By the means of numerical simulation and physical simulation, the failure laws of overlying strata are uncovered and the optimal caving ratios for preventing water-inrush are defined (Chen et al. 2007). Combining numerical simulation, the field experiment shows that water-inrush is caused by the compound breakage of key strata induced by the load transfer of the unconsolidated and confined aquifer (Xu et al. 2011; Wang et al. 2012). By physical simulation, the initial water head of the aquifer and the style of water-conducting fracture are considered to be important factors controlling water-inrush (Sui et al. 2007). As can be seen from above, the studies of water-inrush under the unconsolidated and confined aquifer have been progressed by the theoretical analysis, numerical simulation, physical simulation and field experiment.

The water-conducting fracture is the fracture which is produced in the overlying strata of the working face during mining and groundwater seepage can easily occur through the water-conducting fracture. It is obvious that the disastrous water will rush out from the unconsolidated and confined aquifer through the water-conducting fracture in overlying strata if the fracture extends to the aquifer in process of mining (Zhang et al. 2015). However, there are complex geological and hydrogeological conditions influencing the development of the water-conducting fracture, especially in the eastern mine areas in China. The geological and hydrogeological conditions are usually defined by main factors such as the water yield and water pressure in the aquifer, the structure of overlying strata, the fault distribution and so on (Zhang et al. 2009, 2015; Huang et al. 2012). Therefore, relevant researches on water-inrush under the unconsolidated and confined aquifer have its limitations and may be in no agreement with the complex geological and hydrogeological conditions.

The Qidong coal mine lays in Huaibei coalfield, one of the eastern mine areas in China, where coal seams are covered by the unconsolidated and confined aquifer. It is so rare that strong water yield and high water pressure in the aquifer, the special structure of the overlying strata and the complex fault distribution occur simultaneously in the Qidong coal mine, which is divided into two mining areas by the Weimiao fault: the south mining area and the north mining area. In the north mining area, most of working faces have been mined and at least 18 water-inrush hazards from the aquifer have happened (Wang 2012; Xu et al. 2011). In the south mining area, some working faces have begun to mine. Similar to the north mining area, mining in the south mining area begins to face the danger of water-inrush. On the basis of mass mining data collected in the north mining area, the engineering analogy method is applied to predict the water-inrush risk areas in the south mining area by Fisher's discriminant analysis, which considers synthetically these complex geological and hydrogeological conditions and certainly will contribute to the subsequent mining in the Qidong coal mine.

Geological settings

The Huaibei coalfield (Fig. 1), one of the eastern mine areas in China, locates in northern Anhui province and borders between the nearly EW trend Fengpei uplift and

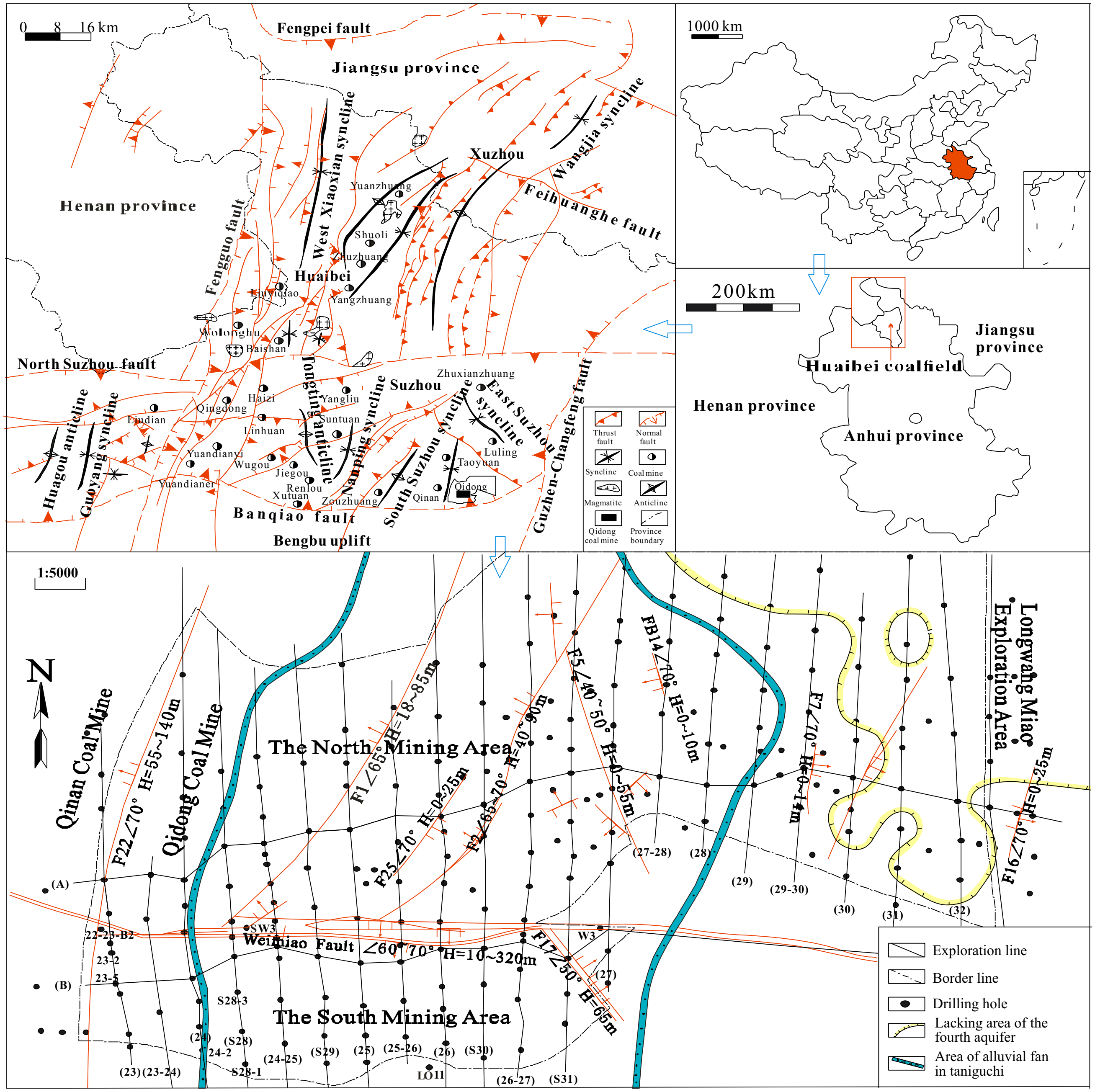

Fig. 1 Diagram of regional tectonic structure in the Huaibei coalfield (Wang et al. 2013; Guo et al. 2014)

the Bengbu uplift. The main structural units are controlled by the EW and NNE trend faults and the NNE or NE and NW trend folds (Tan et al. 2011). The EW trend faults mainly include the north Suzhou fault and the Banqiao fault, and the NNE trend faults mainly include the Fengguo fault and the Guzhen-Changfeng fault. The NNE or NE trend folds include the Huagou anticline, the Guoyang syncline, the Nanping syncline, the south Suzhou syncline etc., and the NW trend folds include the Tongting anticline and the East Suzhou syncline. Most coal mines in the Huaibei coalfield are suffering from the risk of water-inrush in process of mining under the unconsolidated and confined aquifer. The study area—the Qidong coal mine, which shows meaningful typicality and reference, locates in the south Suzhou syncline in the Huaibei coalfield.

The Qidong coal mine (Fig. 1), with 35 km^2 in area, is one of the biggest coal mines in Huaibei coalfield, and locates next to the Longwangmiao exploration area and the Qinan coal mine. The general structural feature of the mine is a monoclinal structure with EW trend and N10°–15° dip, following a series of secondary folds and faults (Wu et al. 2010). The type of fault is mainly the NE or NNE trend normal faults with the supplement of the NW trend reverse faults. The EW trend Weimiao fault divides the mine into two parts: the south mining area and the north mining area. The primary mineable coal seams are no. 3_2, 6_1 and 8_2 in the north mining area and no. 6_1, 8_2 and 9 in the south mining area. According to the lithology and the permeability, the unconsolidated Cenozoic formation, which is mainly made up of clay, sandy clay, clayey sand, silt, fine sand, medium sand and gravel et al., can be divided into four aquifers and three aquifuges from up to down: the first aquifer (25–30 m), the first aquifuge (15–25 m), the second aquifer (30–45 m), the second aquifuge (10–30 m), the third aquifer (60–100 m), the third aquifuge (130–180 m) and the fourth aquifer (15–50 m), respectively (Fig. 2). The fourth aquifer, overlaying the coal measure strata directly, is the confined aquifer and the main water-inrush aquifer to the working faces in process of mining in the Qidong coal mine. The water-bearing media of the fourth aquifer is comprised of the pluvial-alluvial deposits and the residual-floodplain deposits. The former deposits distribute in the middle of the mine with the maximum 53.3 m thickness and the latter are located on both sides. The hydrogeological parameter values of the fourth aquifer are determined by the drainage test in the mine. In view of the geological and hydrogeological conditions, the fourth aquifer presents the characteristics of high pressure and strong seepage, and is thought as the unconsolidated and confined aquifer.

Fisher's discriminant analysis

Fisher's discriminant analysis is one of the most widely used methods of dimensionality reduction and classification, and has no special requirement for real geological data. Based on the method of dimensionality reduction, the Fisher's discriminant model can be established by calculating these known sample data. The main idea of Fisher's discriminant analysis is to discriminate the data by means of projection from the multi-dimensional space to the low-dimensional space. The principle of the projection is that each group can be separated as much as possible (Sierra 2002). Then, being submitted into the Fisher's discriminant model, new unknown samples can be well classified and analyzed on the fact that the ratio of between-class variance and within-class variance is maximized (He et al. 2009; Zhang et al. 2008).

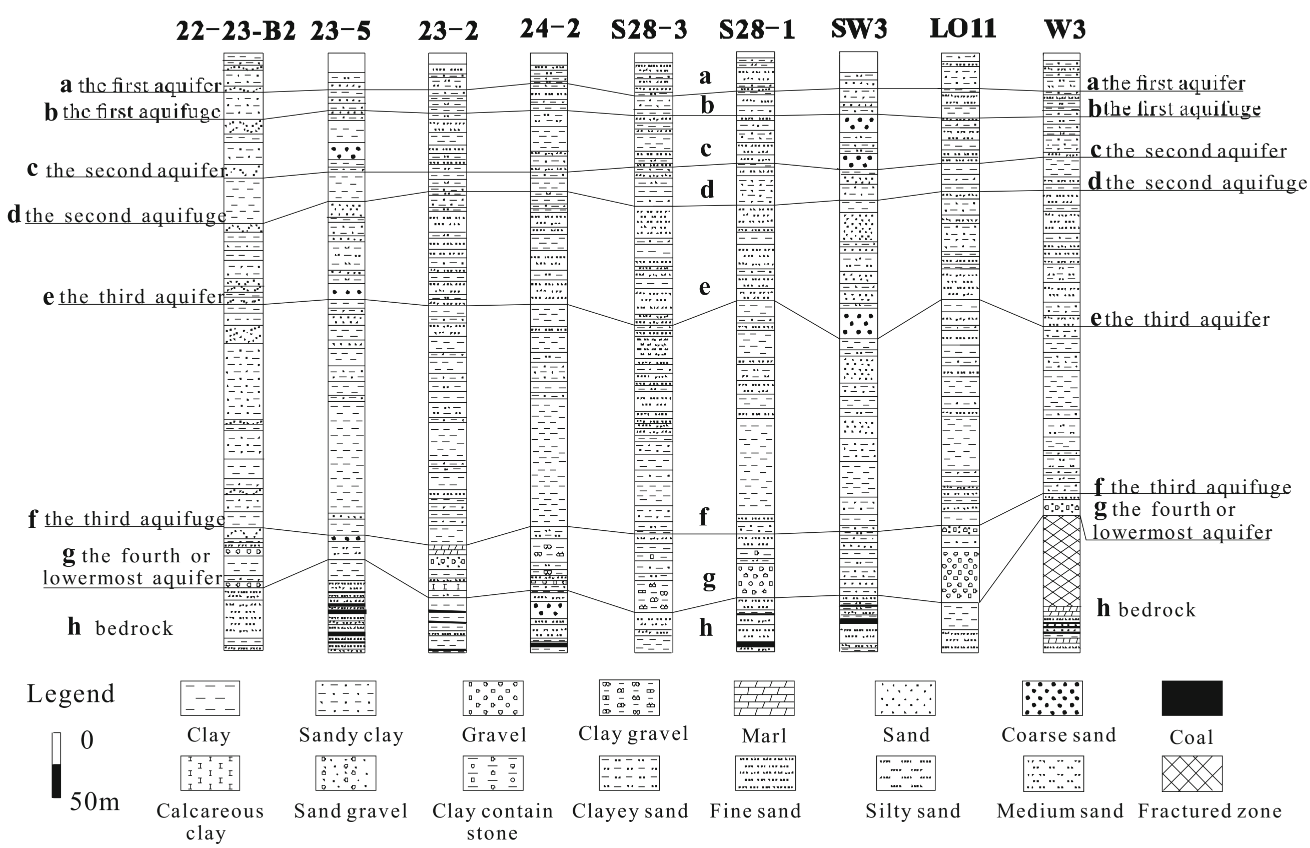

Fig. 2 Stratigraphic column and aquifer division of the fourth aquifer in the Qidong coal mine

Fisher's discriminant analysis plays an important role in overcoming the crucial curse of dimensionality problems and reducing the heavy burden of storage and computation brought by the original high-dimensional data (Ji et al. 2012). It is also practically parameter-free, especially compared with neural networks and other methods. There are no structural parameters to adjust, no learning constants or activation functions to choose and no weight initialization schemes to start learning from (Sierra 2002). Moreover, Fisher's discriminant analysis does not require the distribution type of the choosing samples, so we can fully select some relevant and optional influence factors inducing water-inrush to establish the discriminant model. When the mechanisms of action for the influence factors are not defined, the model has great value in practical application (Liu et al. 2012).

Establishment of the Fisher's discriminant model for water-inrush

Discriminant indexes

Based on the previous research results (Wang 2012; Xu et al. 2012; Huang et al. 2012; Meng et al. 2013) and the special geological and hydrogeological conditions in the Qidong coal mine, six main influence factors inducing water-inrush, including the effective thickness, the specific yield and the load transfer coefficient of the unconsolidated and confined aquifer, the effective thickness of the protective bedrock layer, the fractal dimensional value of bedrock faults and the distance between the key hard stratum and the primary mineable coal seam, are selected as discriminant indexes in the Fisher's discriminant analysis. Discriminant indexes such as the effective thickness, the specific yield and the load transfer coefficient of the unconsolidated and confined aquifer can be precisely calculated for the fourth aquifer, and the other discriminant indexes can be properly estimated on the basis of some theory.

Effective thickness of the unconsolidated and confined aquifer

The unconsolidated and confined aquifer overlaying the coal measure strata is the main water-inrush aquifer in process of mining in the Qidong coal mine. A large effective thickness of the aquifer may incur a great amount of water inflow into the working face once the water-inrush hazard happens. From Fig. 3a, the distribution of the effective thickness is not homogeneous from 0 to 55 m in the Qidong coal mine and the large values of effective thickness lie mainly in pluvial-alluvial deposits.

Specific yield of the unconsolidated and confined aquifer

Specific yield of the unconsolidated and confined aquifer reflects the water-inrush capacity as an important hydrogeological parameter (Bateni et al. 2015; Cheng and Chen 2007). As shown in Fig. 3b, the value of specific yield of the aquifer ranges from 0.01 to 0.400 l/s·m with the decreasing trend from west to east in the Qidong coal mine.

Load transfer coefficient of the unconsolidated and confined aquifer

The load transfer coefficient of the unconsolidated and confined aquifer is the load ratio between the bottom and the top interface, reflecting the degree of load transfer action in the aquifer (Wang 2012). If the load transfer coefficient is great, the load value transferred to the bedrock is great. At this time, the key hard stratum of overlying strata under the aquifer is prone to the compound breakage, which will result in the water-inrush hazard. Assuming that the aquifer is saturated and plastically deformed, the equation of the load transfer coefficient is shown as follows (Wang 2012):

$$k_z = [\gamma_{\mathrm{w}} H' + k(\gamma H + \gamma_{\mathrm{sat}} h - \gamma_{\mathrm{w}} H')]/\gamma H \quad (1)$$

where k_z is the load transfer coefficient; H is the distance between the ground surface and the aquifer, m; γ is the average bulk density of layers between the ground surface and the aquifer, kN/m^3; H' is the height of water head in the aquifer, m; γ_{w} is the average bulk density of water, kN/m^3; h is the thickness of the aquifer, m; γ_{sat} is the average bulk density of the aquifer, kN/m^3; k is the transfer coefficient of effective stress. According to the practical mining situation in the Qidong coal mine, the value of k is taken as 0.5 (Wang 2012).

As shown in Fig. 3c, the load transfer coefficient of the aquifer in the Qidong coal mine is not homogeneous, ranging from 0.76 to 0.85 with an increment from side to middle in the mine.

Effective thickness of the protective bedrock layer

The effective thickness of the protective bedrock layer is an important discriminant index to judge whether the water-conducting fracture in overlying strata can conduct the unconsolidated and confined aquifer (Meng et al. 2013). The equation of the effective thickness is as follows:

$$H_{\mathrm{e}} = \Delta H - H_{\mathrm{li}} \quad (2)$$

where H_{e} is the value of effective thickness of the protective bedrock layer, m; ΔH is the distance between the coal seam and the aquifer, m; H_{li} is the height of water-

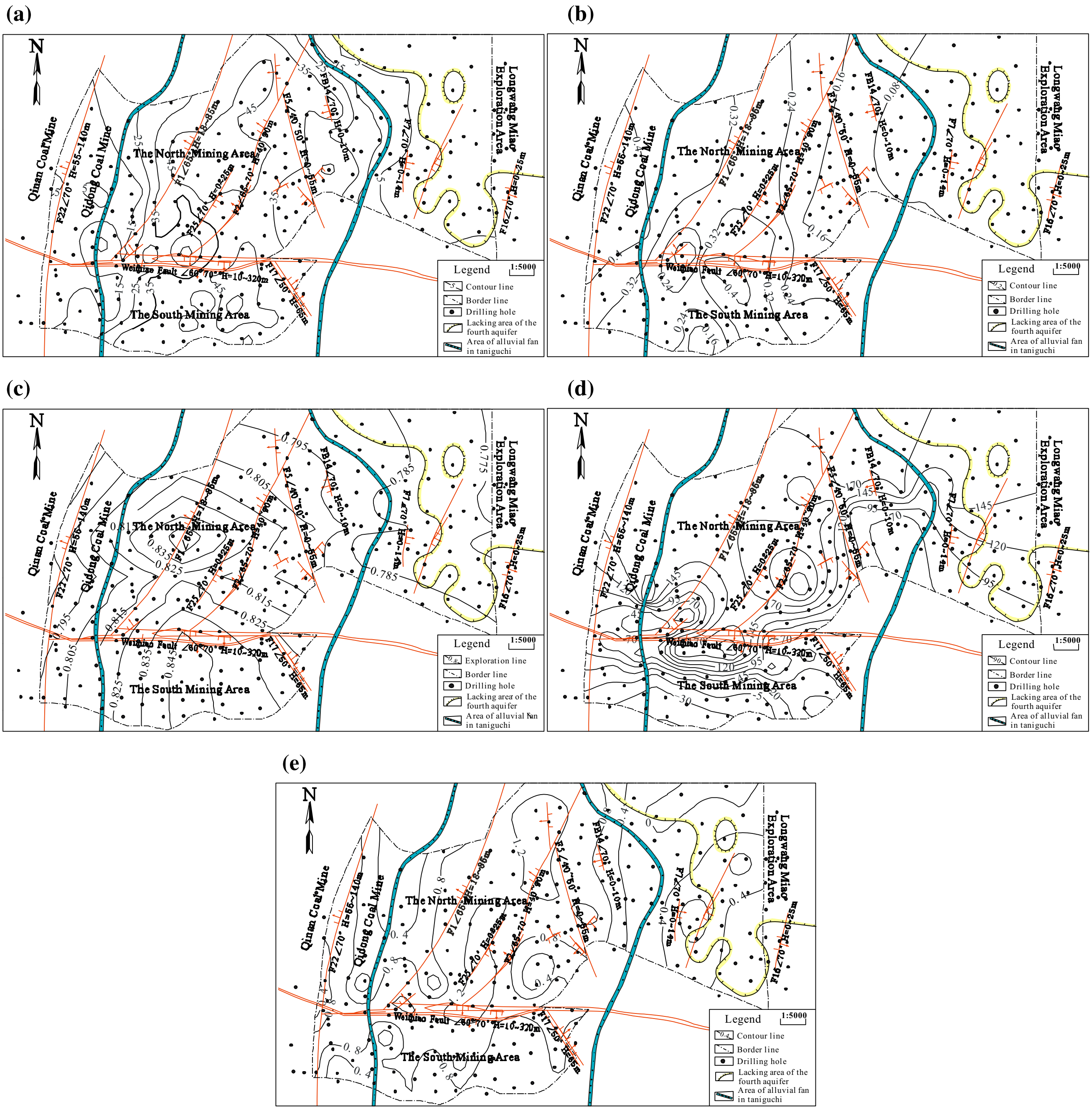

Fig. 3 Contour maps of discriminant indexes in the Qidong coal mine: **a** effective thickness of the unconsolidated and confined aquifer; **b** specific yield of the unconsolidated and confined aquifer; **c** the load transfer coefficient of the unconsolidated and confined aquifer; **d** effective thickness of the protective bedrock layer of no. 6_1 coal seam; **e** fractal dimensional value of bedrock faults

conducting fracture zone, being taken as ten times mining height of the coal seam (Xu et al. 2012).

The value of effective thickness of the protective bedrock layer of no. 6_1 coal seam (Fig. 3d) generally decreases from north to south. The minimum is located in the south of the south mining area due to some lack of area of no. 6_1 coal seam, and the maximum is in the middle in the north mining area.

Fractal dimensional value of bedrock faults

The word "fractal" is first put forward by Mandelbrot and Wheeler (1982). The fractal dimension of bedrock faults, which can quantitatively describe the irregularity of bedrock faults, is more accurate than other indexes such as fault density, and its value is more reflective to the complexity degree of bedrock faults as a discriminant index (Li

Table 1 Discriminant result for the key hard stratum of overlying strata in S30-3 drilling hole

No.	Lithology	Depth (m)	Thickness (m)	Unit weight (kN/m^3)	Elastic modulus (Gpa)	Compressive strength (Mpa)	Location of hard stratum	Location of key hard stratum
15	Unconsolidated layer	398.8	398.8	0.018	0	0		
14	Medium sand	411.5	12.7	0.0234	30	32	Hard stratum	
13	Clay	420.67	9.17	0.0202	15	28		
12	Coal	421.67	1	0.0135	12	11		
11	Clay	422.9	1.23	0.0202	15	28		
10	Silty sand	426.5	3.6	0.024	34	35		
9	Clay	439.1	12.6	0.0202	15	28		
8	Fine sand	446.8	7.7	0.0247	45	44		
7	Clay	452	5.2	0.0202	15	28		
6	Fine sand	454.5	2.5	0.0247	45	44		
5	Clay	470.1	15.6	0.0202	15	28		
4	Fine sand	483.46	13.36	0.0247	45	44	Hard stratum	Key hard stratum
3	Coal	483.63	0.17	0.0135	12	11		
2	Clay	484.82	1.19	0.0202	15	28		
1	No. 6_1 coal	486.58	1.76	0.0135	12	11		

et al. 2015). The small value means the wide and dispersed distribution of bedrock faults, and the big value means the complex structure and the intensive distribution of bedrock faults, which will have a bad effect on the safe mining of coal seams. The fractal dimensional value of bedrock faults in the Qidong coal mine is calculated by the box-counting method (He et al. 2014; Li et al. 2012) in fractal dimension theory. From Fig. 3e, due to the irregular distribution of bedrock faults, the fractal dimensional value of bedrock faults in the Qidong coal mine is not homogeneous from 0.4 to 1.2, which maximum mainly distributes in the areas near the large bedrock faults such as the Weimiao fault.

Distance between the key hard stratum and the primary mineable coal seam

As lithology and thickness are different, the mechanical effect of each stratum is also different. Some hard and thick strata have controlling effect on deformation and failure, which are called the key hard strata (Yu 2009). The deformations of the whole or partial strata above the key stratum are synchronized with the deformation of the key hard stratum (Miao et al. 2011). If the distance between the key hard stratum and the primary mineable coal seam is shorter than a certain value, the key hard stratum is prone to the compound breakage, resulting in the water-inrush hazard in process of mining under the unconsolidated and confined aquifer.

The key hard stratum is judged by the load discriminant condition (Formula 3) and the strength discriminant condition (Formula 4). The discriminant result for the key hard stratum of overlying strata in S30-3 drilling hole is seen in Table 1.

$$\sum_{i=i}^{n} E_i h_i^3 \sum_{i=i}^{s} \gamma_i h_i < \sum_{i=i}^{n+1} E_i h_i^3 \sum_{i=i}^{n} \gamma_i h_i \quad (3)$$

$$l_1 < l_{n+1} \quad (4)$$

where E_i is the elastic modulus in the ith layer, GPa; h_i is the thickness in the ith layer, m; γ_i is the bulk density in the ith layer, kN/m^3; l_i is the breaking interval of the hard stratum in the ith layer, m.

Types of water-inrush risk areas in the north mining area

Based on the amount of water inflow in process of mining, the water-inrush risk areas under the unconsolidated and confined aquifer in the Qidong coal mine can be divided into three types. Type 1 is the safety area with water inflow ranging from 0 to 50 m^3/h, Type 2 is the medium risk area with water inflow ranging from 50 to 300 m^3/h, and Type 3 is the risk area with water inflow exceeding 300 m^3/h. The water-inrush hazard doesn't usually happen where the thickness of bedrock is more than 125 m (Wang 2012), so the corresponding water-inrush risk area can be incorporated into Type 1 except in special cases. Types of water-inrush risk areas in the north mining area of the Qidong coal mine, following the information of drilling holes, are listed in Table 2, where

Table 2 Types of water-inrush risk areas and the information of drilling holes in the north mining area of the Qidong coal mine

No.	Working face	Drilling hole	Thickness of bedrock (m)	Maximum water inflow (m^3/h)	Type
1	$7_1$12	26-27-9	154.70	47.6	1
		26-27-18	246.65		1
2	$7_1$14	26-27-8	128.72	169	2
		S31-8	250.56		1
		S31-15	208.52		1
3	$7_1$15	S31-14	178.02	16.7	1
		S31-8	250.56		1
		S31-7	127.11		1
4	$7_1$20	24-25-15	71.35	50	2
5	$7_1$21	24-25-7	103.85	52	2
		25-5	94.39		2
		92-1	103.45		1
		S29-6	114.22		2
6	$7_1$23	25-26-6	192.09	14	1
7	$7_1$24	25-7	230.75	14	1
8	$7_1$30	B1	54.63	850	3
		B2	43.61		3
		29-30-2	76.58		3
		30-3	116.90		1
		H91	68.54		3
9	$7_1$31	B3	76.16	300	3
		28-4	99.87		3
10	$6_1$12	26-27-18	198.60	0	1
11	$6_1$13	S31-15	163.29	10	1
12	$6_1$14	S31-8	196.00	26	1
13	$6_1$15	S31-14	142.58	38	1
14	$6_1$30	28-4	52.14	500	3
		B3	50.13		3
		H10-2	94.84		3
15	$6_1$33	30-4	171.05	20	1
16	$6_1$34	27-7	87.21	51	2
17	$6_1$35	29-30-3	177.40	35.9	1
		28-6	191.91		1
18	$6_1$36	27-28-4	190.34	5	1
		27-8	193.46		1
		S31-11	260.32		1
19	$6_1$37	29-4	116.05	10	1
20	$6_1$63	24-25-2	214.50	6.9	1
		S29-4	215.20		1
		25-4	231.67		1
21	$3_2$21	26-11	119.75	238.5	2
22	$3_2$22	26-5	57.06	1520	3
23	$3_2$24	25-26-9	202.67	53	1
		25-26-8	103.59		2
24	$3_2$26	25-11	206.39	2	1
		25-8	143.06		1
25	$3_2$41	S28-8	102.95	54	2
		24-25-4	94.71		2
26	$3_2$44	24-7	136.70	27	1

Table 2 continued

No.	Working face	Drilling hole	Thickness of bedrock (m)	Maximum water inflow (m^3/h)	Type
27	3_245	S29-8	218.49	5	1
		24-25-5	251.53		1
		S28-9	253.03		1
28	3_246	24-8	282.68	40.6	1
29	8_223	24-25-7	138.12	4.5	1
		25-5	127.80		1
		S29-6	149.93		1
30	8_224	S29-7	273.87	40	1

1, 2 and 3 represent the safety area, the medium risk area and the risk area, respectively.

Training samples

From Table 2, 52 drilling holes in the north mining area are selected as the training samples. The training sample data are shown in Table 3, where the discriminant indexes from x_1 to x_6 represent the effective thickness, the specific yield and the load transfer coefficient of the unconsolidated and confined aquifer, the effective thickness of the protective bedrock layer, the fractal dimensional value of bedrock faults and the distance between the key hard stratum and the primary mineable coal seam, respectively.

Establishment of Fisher's discriminant model

According to the training sample data (Table 3), the discriminant functions for water-inrush are gotten by Fisher's discriminant analysis method, which are seen as follows:

$$y_1 = -0.022x_1 - 3.847x_2 - 0.082x_3 + 0.027x_4 + 1.724x_5 + 0.044x_6 - 3.970 \quad (5)$$

$$y_2 = -0.035x_1 + 5.267x_2 + 30.312x_3 - 0.002x_4 + 0.944x_5 - 0.014x_6 - 25.005 \quad (6)$$

The variances of discriminant functions and their significances refer to Table 4. From Table 4, the first discriminant function (Eq. 5) can explain most information of the training samples with the 90.0 % variance contribution, but cannot explain all the information of samples until it is combined with the second discriminant function (Eq. 6). From Table 5, the coordinate values at group centroids are (1.160, −0.053) in the safety area, (−2.054, 0.922) in the medium risk area and (−2.865, −1.051) in the risk area, respectively. Therefore, a new sample can be discriminated by comparing the distance between single sample value and the group centroid value.

Discussions

Test for the discriminant model

For the purpose of testing the discriminant model's accuracy and classified effect, fifty-two training samples in the north mining area of the Qidong coal mine are substituted into the discriminant model. By comparison between the predicted types and the actual types of training samples, it is found that there are five fault discriminant samples (Table 3), and the correct discriminant ratio is 47/52 = 90.4 %, reflecting the discriminant model's high accuracy. From Table 6, the Wilks' Lambda values of two discriminant functions (0.000 and 0.020) are below the significant level $\alpha = 0.05$, showing that the discriminant model is significant. According to the scatter diagram of training samples (Fig. 4), the deviation between single sample value and the group centroid value is small and the deviation among group centroid values is big, showing a good cluster degree and classified effect.

From the back substitution of training samples, the significance test and the scatter analysis, the Fisher's discriminant model for water-inrush is accurate and can be properly applied to predict the water-inrush risk areas in process of mining under the unconsolidated and confined aquifer, so that different water-inrush risk areas including the safety area, the medium risk area and the risk area can be classified apparently.

Prediction for water-inrush risk areas in the south mining area

Because the south mining area has the same conditions as the north mining area in the Qidong coal mine, the engineering analogy method can be applied to predict the water-inrush risk areas under the unconsolidated and confined aquifer in the south mining area by the Fisher's discriminant model. By the data of x_1–x_6 of drilling holes in the mining area, the discriminant types of water-inrush risk

Table 3 Training samples and their actual and prediction types

No.	Drilling hole	Primary coal seam	x_1	x_2	x_3	x_4	x_5	x_6	Actual type	Predicted type
1	25-26-9	3_2	53.3	0.3	0.844	177.37	1.16	34.27	1	1
2	26-5	3_2	45.8	0.27	0.848	28.06	1.21	7.37	3	2[a]
3	25-11	3_2	52.8	0.31	0.853	175.99	1.05	3.69	1	1
4	24-25-4	3_2	11.0	0.33	0.801	70.17	0.65	0.00	2	2
5	25-26-8	3_2	50.0	0.29	0.840	73.99	1.22	26.94	2	2
6	25-8	3_2	53.0	0.31	0.846	112.66	1.10	17.36	1	2[a]
7	26-11	3_2	50.1	0.26	0.848	67.00	1.22	6.52	2	2
8	S28-8	3_2	9.1	0.36	0.780	78.55	0.45	0.00	2	2
9	24-7	3_2	14.0	0.40	0.787	110.6	0.55	34.90	1	1
10	S29-8	3_2	41.2	0.33	0.831	194.99	0.64	11.73	1	1
11	24-25-5	3_2	2.4	0.35	0.792	223.43	0.17	6.63	1	1
12	S28-9	3_2	6.5	0.37	0.785	227.73	0.10	56.29	1	1
13	24-8	3_2	5.3	0.39	0.759	259.78	0.45	2.88	1	1
14	B3	6_1	19.0	0.03	0.792	25.00	0.30	10.16	3	3
15	26-27-18	6_1	41.0	0.19	0.816	176.10	1.22	0.00	1	1
16	S31-8	6_1	38.4	0.15	0.814	173.00	1.17	2.65	1	1
17	S31-14	6_1	34.9	0.2	0.815	121.38	1.23	49.78	1	1
18	28-4	6_1	21.8	0.04	0.786	40.74	0.35	0	3	3
19	30-4	6_1	1.97	0.01	0.768	136.85	0.72	13.75	1	1
20	27-7	6_1	33.7	0.11	0.807	69.71	1.07	0.00	2	2
21	29-30-3	6_1	3.9	0.01	0.774	150.10	0.40	20.69	1	1
22	28-6	61	21.8	0.01	0.791	177.51	0.24	0.00	1	1
23	27-8	6_1	33.7	0.12	0.806	175.46	0.96	0.00	1	1
24	S31-11	6_1	37.1	0.16	0.817	242.72	0.50	5.62	1	1
25	29-4	6_1	11.8	0.03	0.770	95.35	0.05	36.60	1	1
26	24-25-2	6_1	37.7	0.30	0.836	194.7	1.10	16.80	1	1
27	S29-4	6_1	37.6	0.38	0.839	195.5	1.10	40.26	1	1
28	25-4	6_1	36.2	0.42	0.846	212.97	1.00	0.00	1	1
29	H10-2	6_1	1.96	0.04	0.765	83.64	0.65	0.00	1	3[a]
30	27-28-4	6_1	44.0	0.09	0.824	165.64	0.55	26.10	1	1
31	25-7	7_1	29.4	0.31	0.822	206.9	1.00	27.35	1	1
32	26-27-8	7_1	39.9	0.16	0.857	45.00	0.80	0.00	2	2
33	S31-15	7_1	38.0	0.16	0.820	194.62	1.20	0.00	1	1
34	29-30-2	7_1	4.0	0.02	0.774	37.58	0.60	0.47	3	3
35	26-27-9	7_1	42.5	0.17	0.822	128.3	1.10	10.00	1	1
36	26-27-18	7_1	43.0	0.19	0.816	231.05	1.23	5.15	1	1
37	S31-14	7_1	38.6	0.20	0.815	133.82	1.22	2.92	1	1
38	S31-8	7_1	38.4	0.15	0.815	233.46	1.17	2.16	1	1
39	S31-7	7_1	39.3	0.14	0.812	113.01	1.13	28.84	1	1
40	24-25-15	7_1	41.0	0.14	0.841	48.15	1.06	0.00	2	2
41	24-25-7	7_1	25.6	0.30	0.827	75.85	1.02	0.00	2	2
42	25-5	7_1	37.7	0.34	0.830	69.79	1.10	10.94	2	2
43	S29-6	7_1	46.7	0.27	0.848	87.42	1.03	2.72	2	2
44	25-26-6	7_1	42.9	0.31	0.836	168.69	1.23	13.59	1	1
45	B1	7_1	2.0	0.01	0.770	12.63	0.75	0.00	3	3
46	B2	7_1	6.0	0.01	0.764	4.81	0.35	3.32	3	3
47	H9-1	7_1	13.9	0.02	0.769	27.74	0.10	3.8	3	3
48	30-3	7_1	1.9	0.02	0.763	76.90	1.00	2.64	1	1

Table 3 continued

No.	Drilling hole	Primary coal seam	x_1	x_2	x_3	x_4	x_5	x_6	Actual type	Predicted type
49	24-25-7	8_2	25.6	0.25	0.827	111.62	1.03	0.00	1	2[a]
50	25-5	8_2	37.7	0.34	0.830	102.10	1.11	44.35	1	1
51	S29-6	8_2	46.7	0.28	0.848	123.43	1.03	12.93	1	2[a]
52	S29-7	8_2	44.3	0.31	0.840	245.87	0.94	0.80	1	1

[a] False discriminant type

Table 4 Variances of discriminant functions and their significances

Function	Eigenvalue	Variance contribution %	Cumulative variance contribution %	Canonical correlation
1	2.994	90.0	90.0	0.866
2	0.333	10.0	100	0.500

Table 5 Values of discriminant functions at group centroids

Type	Function 1	Function 2
Safety area	1.160	−0.053
Medium risk area	−2.054	0.922
Risk area	−2.865	−1.051

Table 6 Wilks' lambda test

Test of function	Wilks' lambda	Chi square	Degree of freedom	Significance
1 through 2	0.188	77.760	12	0.000
2	0.750	13.371	5	0.020

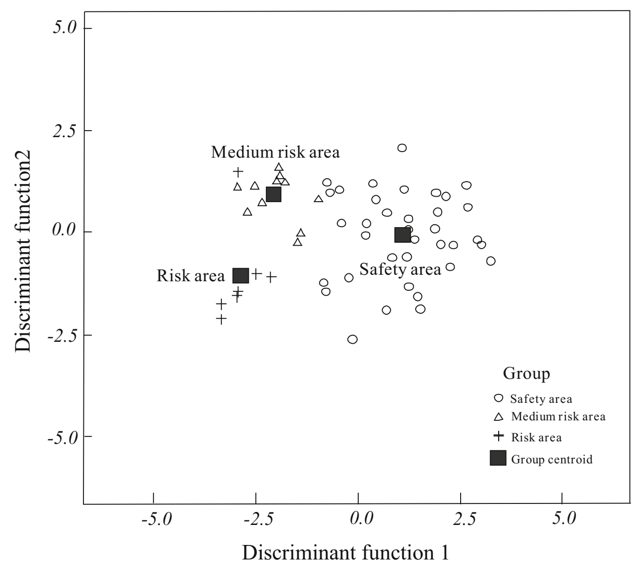

Fig. 4 Scatter diagram of training samples

areas for no. 6_1, 8_2 and 9 primary mineable coal seams are shown in Tables 7, 8, 9.

Based on the Fisher's discriminant results of no. 6_1, 8_2, and 9 primary mineable coal seams in the south mining area, water-inrush risk areas of each coal seam in the mining area are denoted in Fig. 5. From Fig. 5, the three types including the safety area, the medium risk area and the risk area, in general, are distributed orderly from north to south. The safety area is located in the north of the mining area where the thickness of bedrock is large, the risk area is located in the south of the mining area where the coal seam outcrop appears, and the medium risk area lies between the safety area and the risk area.

Field verification in the south mining area

The no. $6_1$63 first working face in the south mining area lies between the 24–25 exploration line and the 25 exploration line, with −527 to −610 m in elevation, 1100 m in the strike direction and 180 m in the dip direction. By far, in the process of practical mining in no. $6_1$63 working face, the water-inrush hazard under the fourth aquifer hasn't taken place, which is consistent with the predicted type by the Fisher's discriminant model (Fig. 5a).

Therefore, the Fisher's discriminant model is well applied in the engineering analogy method. The predicted water-inrush risk areas by the model will be in accord with

Table 7 Fisher's discriminant result for no. 6_1 coal seam in the south mining area

Drilling hole	x_1	x_2	x_3	x_4	x_5	x_6	Predicted type	Discriminant value of function 1	Discriminant value of function 2
23-11	4.9	0.39	0.795	94.29	1.00	0.0	2	−1.347	1.713
23-2	9.8	0.38	0.800	80.77	1.00	0.0	2	−1.787	1.670
23-5	14.2	0.38	0.787	13.86	0.90	0.0	2	−3.882	1.174
23-24-4	19.3	0.31	0.804	110.2	0.90	4.57	2	−0.899	0.865
24-10	6.5	0.27	0.814	0.00	0.70	0.0	2	−4.546	1.567
24-4	3.8	0.278	0.805	40.61	0.52	0.0	2	−3.185	1.129
24-25-2	37.7	0.265	0.858	194.7	1.10	16.8	1	−4.168	1.209
24-25-6	29.6	0.259	0.838	29.44	0.86	1.39	2	2.045	1.448
25-2	35.63	0.38	0.855	36.94	1.20	0.0	2	−3.346	1.452
25-4	36.18	0.425	0.854	211.87	1.04	22.67	1	−3.216	2.718
25-26-11	45.9	0.40	0.864	142.86	1.14	14.29	2	2.086	2.043
25-26-3	44.5	0.41	0.859	14.58	0.91	1.08	2	−0.112	2.242
26-2	50.12	0.34	0.868	0.00	0.30	2.94	2	−4.592	2.447
26-4	58.1	0.32	0.877	41.19	0.59	0.42	2	−5.817	1.584
26-8	41.36	0.30	0.849	43.3	0.88	6.2	2	−4.404	1.692
26-27-16	47.3	0.20	0.844	55.51	1.05	0.0	2	−3.143	1.509
26-27-17	47.9	0.199	0.846	36.85	1.13	1.9	2	−2.534	0.846
26-27-2	36.8	0.25	0.844	17.17	0.20	0.0	3	−2.832	0.970
26-27-3	38.2	0.21	0.836	84.43	0.30	0.0	2	−5.005	0.759
26-27-4	42.9	0.31	0.866	58.44	0.18	0.0	2	−2.874	0.204
DT1	33.3	0.21	0.864	215.70	1.02	19.4	1	−4.281	1.419
S28-10	22.7	0.199	0.864	106.72	1.15	0.0	2	2.902	1.335
S28-3	22.3	0.245	0.837	35.87	0.75	0.0	2	−0.416	2.290
S28-4	15.4	0.22	0.837	161.45	0.99	20.25	1	−3.205	1.506
S29-3	44.9	0.30	0.838	73.46	0.88	0.0	2	1.771	1.273
S29-4	37.6	0.38	0.865	195.56	1.10	40.26	1	−2.668	1.075
S30-3	54.3	0.218	0.875	67.06	0.07	1.36	2	2.652	1.927
HI4	40.2	0.30	0.850	102.49	0.49	0.0	2	−4.077	0.666
SW3	17.8	0.20	0.840	52.02	1.15	13.8	2	−2.445	1.172

the practical mining of the working faces in the south mining area, and will contribute to the subsequent mining in the mining area in the Qidong coal mine.

Conclusions

The engineering analogy method is used to predict the water-inrush risk areas in process of mining under the unconsolidated and confined aquifer by Fisher's discriminant analysis, and six main influence factors including the effective thickness, the specific yield and the load transfer coefficient of the aquifer, the effective thickness of the protective bedrock layer, the fractal dimensional value of bedrock faults and the distance between the key hard stratum and the primary mineable coal seam (x_1–x_6) are selected as discriminant indexes. The Fisher's discriminant model for water-inrush is established by the discriminant indexes, which are calculated by the geological and hydrogeological data of drilling holes in the north mining area of the Qidong coal mine. By the significance test, the scatter analysis, the back substitution of training samples and field verification, the Fisher's discriminant model is well applied in the engineering analogy method. The Fisher's discriminant model adopted by applying the data of x_1–x_6 of drilling holes in the south mining area, the water-inrush risk areas are predicted, which contribute to the subsequent mining in the mining area of the Qidong coal mine.

Based on the Fisher's discriminant results, the medium risk area, which lies in the middle of the south mining area of the Qidong coal mine, is found dominant among all the

Table 8 Fisher's discriminant result for no. 8_2 coal seam in the south mining area

Drilling hole	x_1	x_2	x_3	x_4	x_5	x_6	Predicted type	Discriminant value of function 1	Discriminant value of function 2
23-11	4.9	0.39	0.795	151.80	1.00	0.00	1	0.222	1.587
23-2	9.8	0.38	0.800	140.90	1.00	0.00	2	−0.147	1.538
23-5	14.2	0.38	0.787	71.29	0.90	10.6	2	−1.852	0.895
23-24-4	19.3	0.31	0.804	165.20	0.90	0.00	1	0.402	0.811
24-10	6.5	0.27	0.814	55.98	0.70	7.49	2	−2.159	1.293
24-4	3.8	0.278	0.805	107.80	0.52	4.88	2	−1.139	0.911
24-25-6	29.6	0.259	0.838	109.30	0.86	0.49	2	−2.330	1.061
24-25-7	25.6	0.210	0.840	115.60	0.73	0.00	2	−1.206	1.290
25-2	35.63	0.38	0.855	111.20	1.20	0.00	2	−1.002	1.103
25-4	36.18	0.425	0.854	280.60	1.04	70.2	1	−1.190	2.556
25-26-11	45.9	0.40	0.864	180.50	1.14	19.14	1	6.032	1.205
25-26-3	44.5	0.41	0.859	98.51	0.91	0.00	2	1.127	2.089
26-2	50.12	0.34	0.868	49.83	0.30	0.00	2	−2.349	2.279
26-4	58.1	0.32	0.877	79.17	0.59	11.13	2	−4.585	1.517
26-8	41.36	0.30	0.849	94.31	0.88	5.15	2	−2.900	1.454
26-27-16	47.3	0.20	0.844	126.10	1.05	0.00	2	−1.797	1.412
26-27-17	47.9	0.199	0.846	92.99	1.13	10.04	2	−0.608	0.692
26-27-2	36.8	0.25	0.844	70.54	0.20	20.60	2	−0.945	0.729
26-27-3	38.2	0.21	0.836	146.00	0.30	9.84	2	−2.650	0.344
26-27-4	42.9	0.31	0.866	80.60	0.18	0.00	2	−0.766	−0.074
DT1	33.3	0.21	0.864	240.30	1.02	1.12	1	−3.677	1.370
S28-3	22.3	0.245	0.837	94.01	0.75	4.51	2	2.776	1.546
S28-4	15.4	0.22	0.837	225.30	0.99	8.00	1	−1.421	1.313
S29-3	44.9	0.3	0.838	153.80	0.88	0.00	2	2.977	1.311
S29-4	37.6	0.38	0.865	253.70	1.1	0.00	1	−0.477	0.899
HI4	40.2	0.30	0.850	158.50	0.49	1.87	2	2.482	2.383
24-25-13	38.0	0.20	0.843	184.3	1.15	1.99	1	−0.836	1.022
24-25-9	41.1	0.08	0.848	61.36	1.00	0.00	2	1.446	0.925
25-3	53.6	0.32	0.871	3.36	1.15	0.00	2	−1.862	0.492
S29-2	38.9	0.24	0.847	25.79	0.65	1.49	2	−4.389	2.285
S28-5	12.3	0.2	0.843	56.76	1.25	0.00	2	−3.937	1.108
23-24-2	22.6	0.29	0.818	15.88	0.75	2.20	2	−1.378	2.226
24-1	10.2	0.27	0.820	−23.10	0.80	0.00	2	−3.832	1.171
S28-2	27.62	0.26	0.834	33.01	0.85	0.00	2	−4.554	1.723
25-26-5	53.6	0.34	0.850	84.95	1.15	0.00	2	−3.286	1.396
26-9	39.68	0.31	0.829	−14.50	1.00	0.82	2	−2.237	1.586
S30-2	49.3	0.29	0.858	3.61	0.25	0.00	3	−4.749	1.327
S30-14	46.3	0.23	0.848	74.95	0.65	14.55	2	−5.721	1.038
S30-6	48.8	0.22	0.838	39.27	0.30	0.00	3	−2.152	0.541
26-27-5	50.9	0.31	0.875	39.08	0.25	1.88	2	−4.380	0.030

Table 9 Fisher's discriminant result for no. 9 coal seam in the south mining area

Drilling hole	x_1	x_2	x_3	x_4	x_5	x_6	Predicted type	Discriminant value of function 1	Discriminant value of function 2
23-11	4.9	0.39	0.795	155.03	1.00	0.00	1	0.310	1.580
23-2	9.8	0.38	0.800	150.49	1.00	0.00	1	0.116	1.517
23-5	14.2	0.38	0.787	79.83	0.90	0.00	2	−2.082	1.030
23-24-4	19.3	0.31	0.804	198.70	0.90	0.00	1	1.317	0.737
24-10	6.5	0.27	0.814	87.87	0.70	0.27	2	−1.603	1.328
24-4	3.8	0.278	0.805	88.00	0.52	1.20	2	−1.840	1.008
24-12	29.5	0.36	0.811	81.38	0.85	2.08	2	−2.300	1.036
24-25-6	29.6	0.259	0.838	18.488	0.86	0.00	2	−3.705	1.496
24-5	22.02	0.42	0.795	133.33	0.48	2.43	2	−1.568	0.660
25-2	35.63	0.38	0.855	106.67	1.20	12.67	2	−0.761	2.382
25-4	36.18	0.425	0.854	292.78	1.04	83.81	1	6.959	0.981
25-26-11	45.9	0.40	0.864	208.37	1.14	29.67	1	2.346	1.875
25-26-3	44.5	0.41	0.859	104.06	0.91	12.35	2	−1.659	2.088
26-4	58.1	0.32	0.877	97.30	0.59	25.16	2	−1.794	1.211
26-8	41.36	0.30	0.849	79.47	0.88	0.00	2	−2.427	1.519
26-27-16	47.3	0.20	0.844	167.34	1.05	0.00	1	0.518	0.601
26-27-17	47.9	0.199	0.846	141.16	1.13	28.31	1	1.166	0.359
26-27-4	42.9	0.31	0.866	98.25	0.18	1.99	2	−3.108	1.303
DT1	33.3	0.21	0.864	248.58	1.02	6.98	1	3.258	1.443
S28-3	22.3	0.245	0.837	109.85	0.75	0.00	2	−1.186	1.343
S28-4	15.4	0.22	0.837	231.95	0.99	21.15	1	3.732	1.106
S29-3	44.9	0.30	0.838	131.74	0.88	12.37	2	−0.539	0.769
S29-4	37.6	0.38	0.865	259.15	1.10	12.84	1	3.190	2.185
S30-3	54.3	0.218	0.877	123.08	0.07	26.08	2	−1.470	0.246
HI4	40.2	0.3	0.850	173.43	0.49	12.23	1	0.024	0.839
X2	27.0	0.33	0.810	34.60	0.75	0.00	2	−3.668	0.973
23-24-2	22.6	0.29	0.818	12.34	0.75	0.00	2	−4.025	1.208
24-12	29.5	0.36	0.811	81.38	0.85	11.70	2	−1.880	0.897
24-4	3.8	0.278	0.805	88.00	0.52	17.90	2	−1.111	0.766
24-1	10.2	0.27	0.820	−7.71	0.80	0.59	2	−4.108	1.679
24-25-9	41.1	0.08	0.848	47.41	1.00	0.00	2	−2.242	0.523
24-25-13	38.0	0.20	0.843	189.60	1.15	14.20	1	2.123	0.736
25-3	53.6	0.32	0.871	−1.55	1.15	0.00	2	−4.523	2.296
25-26-5	53.6	0.34	0.850	94.11	1.15	13.36	2	−1.405	1.362
S30-2	49.3	0.29	0.858	44.95	0.25	5.19	2	−4.367	0.868
S30-14	46.3	0.23	0.848	102.15	0.65	31.55	2	−0.669	0.224
24-25-1	37.3	0.16	0.832	−37.14	0.60	0.00	3	−5.461	0.400
S29-2	38.9	0.22	0.847	13.47	0.65	3.87	2	−4.093	0.995

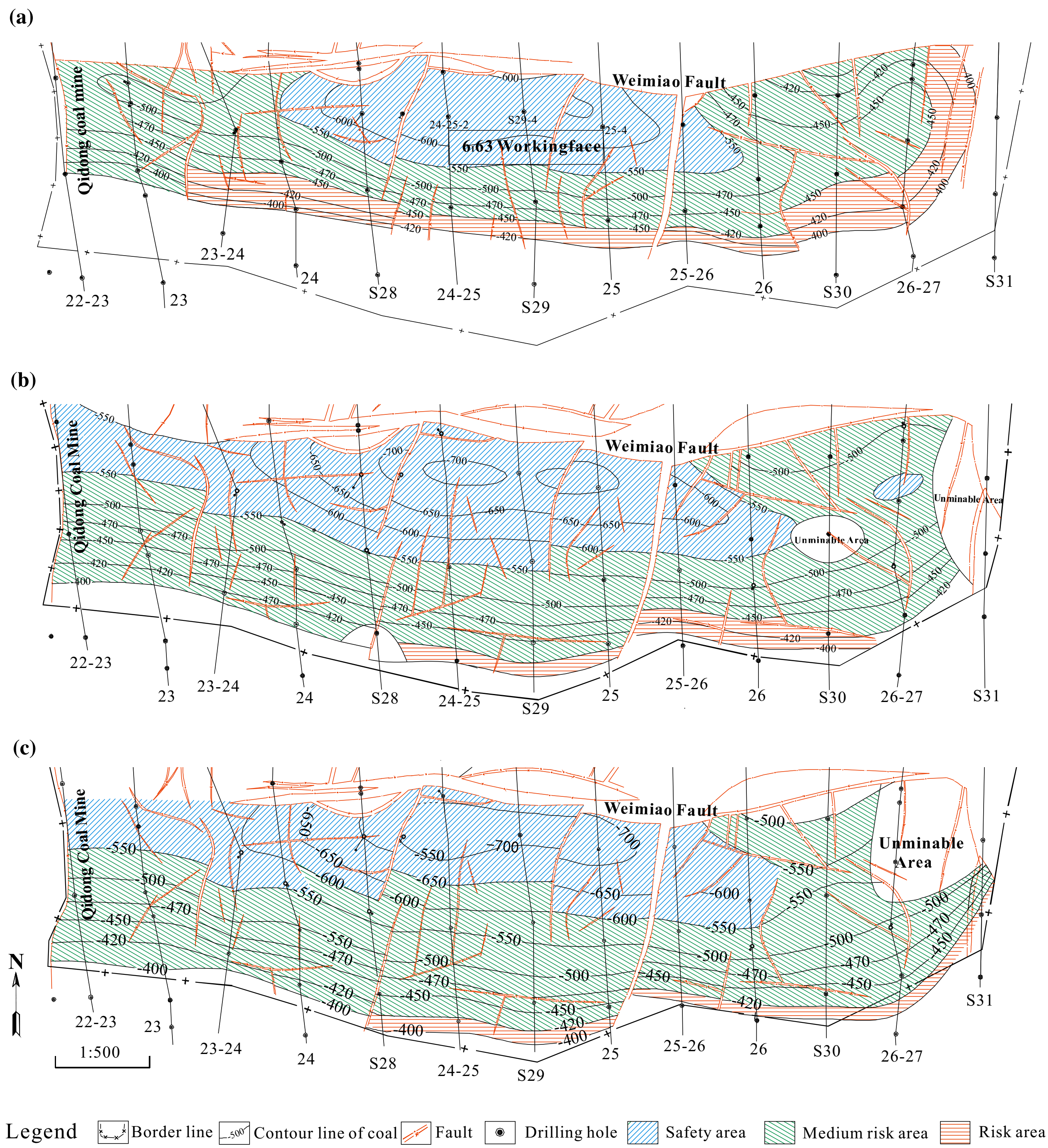

Fig. 5 Water-inrush risk areas of different coal seams in process of mining under the unconsolidated and confined aquifer in the south mining area of the Qidong coal mine: **a** no. 6_1 coal seam; **b** no. 8_2 coal seam; **c** no. 9 coal seam

water-inrush risk areas, and the effective thickness of the protective bedrock layer, the distance between the key hard stratum and the primary mineable coal seam and the fractal dimensional value of bedrock faults are the most important discriminant indexes in determining the types of the water-inrush risk areas.

Acknowledgments This work is financially supported by the National Natural Science Foundation of China (No. 41372244, 41172216, 41373095) and the Anhui Natural Science Foundation of China (No. 1308085ME61). The authors would like to express sincere thanks to the reviewers for their thorough reviews and useful suggestions.

References

Bateni SM, Mortazavi-Naeini M, Ataie-Ashtiani B, Jeng DS, Khanbilvardi R (2015) Evaluation of methods for estimating aquifer hydraulic parameters. Appl Soft Comput 28:541–549

Booth CJ (1986) Strata-movement concepts and the hydrogeological impact of underground coal mining. Ground Water 24(4):507–515

Booth CJ, Bertsch LP (1999) Groundwater geochemistry in shallow aquifers above longwall mines in Illinois, USA. Hydrogeol J 7(6):561–575

Booth CJ, Spande ED (1992) Potentimetric and aquifer property changes above subsiding longwall mine panels, Illinois, USA. Hydrogeol J 7:561–575

Booth CJ, Curtiss AM, Demaris PJ, Bauer RA (2000) Site-specific variation in the potentiometric response to subsidence above active longwall mining. Environ Eng Geosci 6(4):383–394

Chen LW, Gui HR, Li YF (2007) UDEC simulation of the water-pouring probability in exploiting waterproof coal pillars under the conditions of thick loose bed and ultrathin overlying strata. Hydrogeol Eng Geol 34(1):53–56 **(in Chinese)**

Chen LW, Zhang SL, Gui HR (2014) Prevention of water and quicksand inrush during extracting contiguous coal seams under the lowermost aquifer in the unconsolidated Cenozoic alluvium—a case study. Arab J Geosci 7(6):2139–2149

Cheng C, Chen XH (2007) Evaluation of methods for determination of hydraulic properties in an aquifer–aquitard system hydrologically connected to a river. Hydrogeol J 15(4):669–678

Guo PK, Cheng YP, Jin K, Liu YP (2014) The impact of faults on the occurrence of coal bed methane in Renlou coal mine, Huaibei coalfield, China. J Nat Gas Sci Eng 17:151–158

He XB, Wang W, Yang YP, Yang YH (2009) Variable-weighted Fisher discriminant analysis for process fault diagnosis. J Process Contr 19(6):923–931

He ZF, Zhang YN, Guo QC, Zhao XR (2014) Comparative study of artificial neural networks and wavelet artificial neural networks for groundwater depth data forecasting with various curve fractal dimensions. Water Resour Manag 28:5297–5317

Hill JG, Price DR (1983) The impact of deep mining on an overlying aquifer in western Pennsylvania. Ground Water Monit R 3(1):138–143

Huang HF, Mao XB, Yao BH, Pu H (2012) Numerical simulation on fault water-inrush based on fluid-solid coupling theory. J Coal Sci Eng 18(3):291–296

Islam MR, Hayashi D, Kamruzzaman AB (2009) Finite element modeling of stress distributions and problems for multi-slice longwall mining in Bangladesh, with special reference to the Barapukuria coal mine. Int J Coal Geol 78(2):91–109

Ji Z, Jing PG, Yu TS, Su YT, Liu CS (2012) Ranking Fisher discriminant analysis. Neurocomputing 120:54–60

Kim JM, Parizek RR, Elsworth D (1997) Evaluation of fully-coupled strata deformation and groundwater flow in response to longwall mining. Int J Rock Mech Min 34(8):1187–1199

LaMoreaux JW, Wu Q, Zhou WF (2014) New development in theory and practice in mine water control in China. Carbonate Evaporite 29(2):141–145

Li B, Zhang PL, Wang ZJ, Mi SS, Liu PY (2012) Morphological covering based generalized dimension for gear fault diagnosis. Nonlinear Dynam 67(4):2561–2571

Li RZ, Wang Q, Wang XY, Liu XM, Li JL, Zhang YX (2015) Relationship analysis of the degree of fault complexity and the water irruption rate, based on fractal theory. Mine Water Environ. doi:10.1007/s10230-015-0348-2

Liu NP, Wang HT, Yuan ZG, Liu JC (2012) Fisher discriminant analysis model of sand liquefaction and its application. Rock Soil Mech 33(2):554–622 **(in Chinese)**

Mandelbrot BB, Wheeler JA (1982) The fractal geometry of nature. W. H. Freeman and company, San Francisco

Meng ZP, Gao YF, Lu AH, Wang R, Qiao X, Huang CY (2013) Water-inrush risk evaluation of coal mining under Quaternary alluvial water and reasonable design method of waterproof coal pillar. J Min Saf Eng 30(1):23–29 **(in Chinese)**

Miao XX, Cui XM, Wang JA, Xu JL (2011) The height of fractured water-conducting zone in undermined rock strata. Eng Geol 120:32–39

Sierra A (2002) High-order Fisher's discriminant analysis. Pattern Recogn 35(6):1291–1302

Sui WH, Cai GT, Dong QH (2007) Experimental research on critical percolation gradient of quicksand a cross overburden fissures due to coal mining near unconsolidated soil layers. Chin J Rock Mech Eng 26(10):2084–2091 **(in Chinese)**

Tan JQ, Ju YW, Yuan WM, Hou QL, Pan JN, Fan JJ (2011) Thermochronological and structural evolution of the Huaibei coalfield in eastern China: constrains from zircon fission-track data. Radiat Meas 46(2):183–189

Wang XZ (2012) Study on occurrence condition and prevention of support crushing and water-inrush disaster during mining under unconsolidated confined aquifer. Dissertation. China University of Mining and Technology. **(in Chinese)**

Wang XZ, Xu JL, Zhu WB, Li YC (2012) Roof pre-blasting to prevent support crushing and water-inrush accidents. Int J Min Sci Technol 22(3):379–384

Wang HF, Wang L, Cheng YP, Zhou HX (2013) Characteristics and dominant controlling factors of gas outburst in Huaibei coalfeld and its countermeasures. Int J Min Sci Technol 23:591–596

Wu Q, Zhou WF (2008) Prediction of inflow from overlying aquifers into coalmines: a case study in Jinggezhuang Coalmine, Kailuan, China. Envrion Geol 55(4):775–780

Wu SY, Hu BL, Yao DX, Zhang DS (2010) Analysis on geological structures influencing gas occurrence at Qidong coalmine. J Coal Sci Eng 16(3):292–295

Wu Q, Fan ZL, Zhang ZW, Zhou WF (2014) Evaluation and zoning of groundwater hazards in Pingshuo No. 1 underground coal mine, Shanxi Province, China. Hydrogeol J 22(7):1693–1705

Wu Q, Liu YZ, Luo LH, Liu SQ, Sun WJ, Zeng YF (2015) Quantitative evaluation and prediction of water-inrush vulnerability from aquifers overlying coal seams in Donghuantuo coal mine, China. Environ Earth Sci 74:1429–1437

Xu JL, Zhu WB, Wang XZ (2011) Study on water-inrush mechanism and prevention during coal mining under unconsolidated confined aquifer. J Min Saf Eng 28(3):333–339 **(in Chinese)**

Xu JL, Zhu WB, Wang XZ (2012) New method to predict the height of fractured water-conducting zone by location of key strata. J Chin Coal Soc 37(5):762–769 **(in Chinese)**

Yu BH (2009) Study on the hazard-formation mechanism of key strata compound breaking mining under unconsolidated confined aquifer with high water pressure. Dissertation. China University of Mining and Technology. **(in Chinese)**

Zhang JC, Peng SP (2005) Water-inrush and environmental impact of shallow seam mining. Eng Geol 48(8):1068–1076

Zhang JC, Shen BH (2004) Coal mining under aquifers in China: a case study. Int J Rock Mech Min 41(4):629–639

Zhang WJ, Zhong XQ, Liu GH (2008) Recognizing spatial distribution patterns of grassland insects: neural network approaches. Stoch Env Res Risk A 22(2):207–216

Zhang HQ, He YN, Tang CA, Ahmad B, Han LJ (2009) Application of an improved flow-stress-damage model to the criticality assessment of water-inrush in a mine: a case study. Rock Mech Rock Eng 42(6):911–930

Zhang DS, Fan GW, Ma LQ, Wang XF (2011) Aquifer protection during longwall mining of shallow coal seams: a case study in the Shendong Coalfield of China. Int J Coal Geol 86:90–196

Zhang GM, Zhang K, Wang LJ, Wu Y (2015) Mechanism of water-inrush and quicksand movement induced by a borehole and measures for prevention and remediation. B Eng Geol Environ. 74(4):1395–1405